Modeling the potential for thermal concentrating solar power technologies ☆

Yabei Zhang [a], Steven J. Smith [b],*, G. Page Kyle [b], Paul W. Stackhouse Jr.[c]

[a] University of Maryland, Joint Global Change Research Institute and Department of Agricultural and Resource Economics, Symons Hall, Room 2200, College Park, MD 20742, USA
[b] Pacific Northwest National Laboratory, Joint Global Change Research Institute, 5825 University Research Court, Suite 3500, College Park, MD 20740, USA
[c] NASA Langley Research Center, 21 Langley Boulevard, MS 420, Hampton, VA 23681, USA

ABSTRACT

In this paper we explore the tradeoffs between thermal storage capacity, cost, and other system parameters in order to examine possible evolutionary pathways for thermal concentrating solar power (CSP) technologies. A representation of CSP performance that is suitable for incorporation into economic modeling tools is developed. We also combined existing data in order to estimate the global solar resource characteristics needed for analysis of CSP technologies. We find that, as the fraction of electricity supplied by CSP technologies grows, the application of thermal CSP technologies might progress from current hybrid plants, to plants with a modest amount of thermal storage, and potentially even to plants with sufficient thermal storage to provide base load generation capacity. The regional and global potential of thermal CSP technologies was then examined using the GCAM long-term integrated assessment model.

© 2010 Elsevier Ltd. All rights reserved.

1. Introduction

Concentrating thermal solar power (hereafter CSP) technology is a potentially competitive power generation option, particularly in arid regions where direct sunlight is abundant (Emerging Energy Research (EER), 2006). The role of CSP will be determined by its cost relative to other electric generation technologies (National Renewable Energy Laboratory (NREL), 2007a). Although previous studies have projected future CSP costs based on assumptions for technology advancement and the effect of economies of scale and learning curves, few studies have considered the combined effects of intermittency, solar irradiance changes by season, and diurnal and seasonal system load changes (Blair et al., 2006). Because the generation of a solar plant varies over a day and by season, the interactions between CSP generators and other generators in the electric system can play an important role in determining costs. In effect, CSP electricity generation cost will depend on CSP market penetration.

CSP plants either need backup auxiliary generation or storage capacity to maintain electricity supply when sunlight is low or not available. All existing commercially operated CSP plants are hybrid plants (Kearney and Price, 2004). They generally either have a natural-gas-fired boiler that can generate stream to run the turbine, or an auxiliary natural-gas-fired heater for the solar field fluid (Kearney and Price, 2004; National Renewable Energy Laboratory (NREL), 2005), although other fuels such as biomass have also been used. This hybrid structure is an attractive feature of CSP compared to other solar technologies because the auxiliary backup component has a low capital cost and can mitigate intermittency issues to ensure system reliability. The addition of thermal storage would allow better use of available solar energy and would further reduce intermittency issues and potentially lower overall generation costs. However, the cost-effectiveness of adding solar storage depends on the tradeoffs between storage capacity, cost and other CSP system parameters.

CSP technologies have been examined previously. Perhaps the most detailed long-term analysis of this technology is that of Blair et al. (2006) who used a spatially explicit model to examine the potential penetration of CSP in the United States. A number of technologies compete on an economic basis to supply electricity demand. Their model uses CSP capacity factors for each solar resource class and time slice that are constant over time. Hybrid backup operation on low irradiance days does not appear to have been explicitly considered. Fthenakisa et al. (2009) have considered a combination of solar technologies as part of an analysis of the feasibility of supplying a large fraction of US energy demand using solar energy. CSP is included in this analysis, although it appears that fixed capacity factors may have been used to model CSP output. CSP thermal technologies can also be

used for process heat, but this potential is not considered further in this paper (Trieb and Müller-Steinhagen, 2008).

The interaction between CSP generation and the rest of the electric system along with changes in seasonal and daily irradiance make analysis of this technology challenging. This paper examines these relationships and develops a new methodology for representing thermal CSP technologies that can be used in aggregate economic models. Most current analyses of this technology are static, in that economic, and often technology, assumptions are constant over time and penetration level, although seasonal effects are often considered. The representation developed here allows a dynamic representation of this technology to be incorporated into long-term economic analysis. Three applications of CSP technologies are examined: (1) CSP as intermediate and peak (I&P) load power plants without thermal storage, (2) CSP as I&P load power plants with thermal storage, and (3) CSP as base load plants with thermal storage.

We begin in Section 2 with a description of our analytic approach, including the temporal analysis periods and seasonal solar irradiance data used in the analysis. Section 3 provides results for the three CSP applications outlined above. In Section 4 these results are embedded within a long-term, integrated energy-economic model, including a new dataset of global, solar resource data applicable to CSP analysis, to examine the potential role of CSP technologies in the global energy system. We conclude with a discussion.

2. Methodology and assumptions

2.1. Overview

Any long-term analysis of energy systems must strike a balance between technology detail and tractability. Many models that examine time spans 25–100 years into the future operate on an annual average basis often in 5–10 year time steps. In order to facilitate the inclusion of CSP technologies within such long-term analysis, the methodology used here first examines CSP plant operation and its interaction with the electric grid using seasonal average irradiance and electric load distributions, split into ten time slices designed to capture key temporal features. The results are then aggregated to the annual scale appropriate for use in long-term analysis. CSP technologies are considered in two categories: plants supplying intermediate and peak power, and those supplying base load power.

This approach provides a level of detail appropriate for long-term modeling while incorporating key considerations such as changing daily irradiance and load patterns by season. We consider these simplifications reasonable as applied to long-term analysis exercises. More detailed analysis, such as those performed with high temporal resolution dispatch models (Lew et al., 2009), would be warranted for shorter-term planning. Such analysis would also, for example, be able to examine in greater detail the hourly and daily correlations between load and CSP plant output, as well as correlations between CSP output and other renewable resources. These considerations are, however, somewhat less important for CSP plants as compared to, for example PV or wind plants, since the CSP hybrid mode can provide firm power regardless of solar irradiance variations.

2.2. CSP technologies

Three different types of CSP technologies have been developed: (1) parabolic trough, (2) power tower, and (3) parabolic dish. There exist significant design and cost variations among the three technologies. The parabolic trough is currently the most mature and commercially available CSP technology (EERE, 1997; Sargent and Lundy, 2003). This technology uses parabolic trough shaped mirror reflectors to focus the sun's direct beam radiation on a linear receiver located at the focus of the parabola. A heat transfer fluid circulates through the receiver and returns to a series of heat exchangers in the power block where the fluid is used to generate high-pressure superheated steam. The superheated steam is then fed to a conventional reheat steam turbine/generator to produce electricity (EERE, 1997). We focus on this technology and its characteristics in this paper, although most of our insights would also apply to power tower technologies.

For CSP plants without thermal storage, a minimum irradiance level is required for operation. We have assumed a minimum irradiance level of 300 W/m^2 (Kearney and Price, 2004). For CSP plant system efficiencies, we assume constant optical efficiency (ε_{OPT}), heat collector element thermal loss ($Loss_{HCE}$) (W/m^2), solar field piping heat losses ($Loss_{SFP}$) (W/m^2), turbine gross efficiency ($\varepsilon_{turbine}$), and electric parasitic loss ($Loss_{parasitic}$), which means that these parameters do not vary with irradiance level. These parameters are used to formulate the relationships among solar output, solar field size, and direct irradiance level, as expressed in the following equation,[1] where *Asf* is the collecting area of the solar field:

$$Output_{net} = Output_{gross}(1 - Loss_{parasitic})$$
$$= \varepsilon_{turbine} Asf(DNI\varepsilon_{opt} - Loss_{HCE} - Loss_{SFP})(1 - Loss_{parasitic}) \quad (1)$$

In the following sections, we will first detail the methodologies and assumptions used for the case where CSP serves as I&P plants without thermal storage and then discuss the cases with thermal storage.

2.3. Cost components

To calculate the electric generation cost for a CSP plant, we need to consider capital costs, variable costs of running the solar component, and variable costs of running the backup component. Each of these components will be discussed below. Fundamental to this analysis are the load curve for electricity demand and its relationship to solar irradiance, which are described next.

2.4. System load curve and classification of time slices

Electric system load, usually measured in megawatts (MW), refers to the amount of electric power delivered or required at any specific point or points on a system. A system load curve shows the load for each time period considered.

Electric system load can be classified as base load and Intermediate and Peak (I&P) load. While these divisions are somewhat arbitrary, these categories are often used in modeling and serve to capture the difference between plants that operate around the clock and those that operate only during some or all of the day and evening. In principle, base load is the minimum amount of power that a utility must make available to its customers and I&P load as the demand that exceeds base load. Thus base load power plants do not follow the load curve and generally run at all times except for repairs or scheduled maintenance. I&P generation must, in aggregate, follow the load

---

[1] This functional form is from the Solar Advisor Model (SAM) developed by NREL, in conjunction with Sandia National Laboratory and in partnership with the US Department of Energy (reference: personal communication with SAM support staff).

curve. For purposes of the calculation described here base load is considered to be a constant demand during night-time hours not otherwise detailed below (Table 1).

Because the system load curve and CSP electricity output are correlated and both are sensitive to time of day and season, we divide the year into specific time slices and then use these to depict the system load curve. We first define three seasons based on irradiance levels as follows: (1) summer, the three contiguous months with the highest irradiance level; (2) winter, the three contiguous months with the lowest irradiance level; and (3) spring/fall. The classification of time slices is presented in Table 1. The definition of the time slices are chosen for computational convenience to resolve both the load curve and solar irradiance curve, although the exact definitions are not critical other than a requirement that the summer peak should be identifiable as this is a key time period. The assumed system load curve, denoted as $AveSysLoad^i$, is estimated using data from California (California Energy Commission (CEC), 2003) and is shown later in Table 3.

2.5. Solar irradiance data and CSP solar output

CSP solar output depends directly on solar irradiance levels (duration and intensity), solar field size, and system efficiencies. Solar irradiance data is from the National Solar Radiation Data Base (NSRDB; National Renewable Energy Laboratory (NREL), 2007b) and we use Daggett Barstow, California, as an example location to illustrate our analysis. We use the NREL solar data to calculate lowDNIDays, which represents the number of days in a season during which there is not sufficient direct sunlight

to operate the CSP plant, which we take to be days with irradiance below 3000 Wh/m^2/day (or an average of 300 W/m^2 over a 10-hour solar day, Kearney and Price, 2004). We then use this information to adjust NREL's annual direct normal irradiance (DNI) hourly mean data to obtain an estimate of hourly mean DNI value for each month for days during which the CSP plant is operational (Zhang and Smith, 2008). Fig. 1 shows the hourly mean DNI for CSP operational days in Daggett Barstow by season. The annual average daily DNI for operational days is 7.75 kWh/m^2/day.

Because the CSP solar output profile closely follows solar irradiance, we approximate CSP output as solar irradiance times an average net conversion efficiency as described in Eq. (1). For simplicity, we idealize daily solar irradiance as an isosceles trapezoid symmetric about solar noon, as illustrated in Fig. 2. The average daily irradiance, in kWh/m^2/day, is the area of ABFE in Fig. 2.

Given average daily irradiance, noon hours, and daylight hours, we can obtain the maximum irradiance level. We use solar irradiance data described above and obtain the least-squares fit to the hourly mean DNI data by varying noon hours. Once these parameters are determined, we can calculate the daily CSP operational time denoted as $Hour_{CSP}$, the line CD in Fig. 2, which is defined by the minimum operating irradiance for the CSP plant ($MinIrradiance$), assumed to be 300 W/m^2.

Table 1
Classification of time slices.

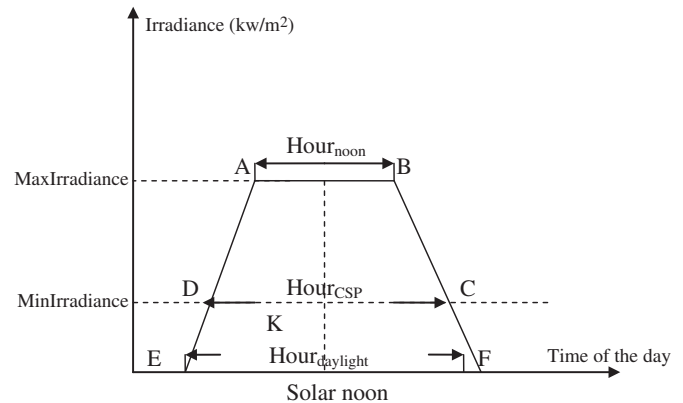| Slice i	Classification of time slices
1	Summer morning (5:00–5:30)
2	Summer daytime 1 (5:30–9:00)
3	Summer daytime 2 (9:00–14:00)
4	Summer peak (14:00–17:00)
5	Summer evening (17:00–24:00)
6	Winter morning (6:00–10:00)
7	Winter daytime (10:00–17:30)
8	Winter evening (17:30–23:00)
9	Spring/fall daytime (5:00–19:30)
10	Spring/fall evening (19:30–22:00)

Fig. 2. Simplified analytic CSP solar output profile by time of the day (not to scale). The trapezoid is defined by the maximum irradiance during the day (MaxIrradiance), daylight hours ($Hour_{daylight}$) and the parameter noon hours ($Hour_{noon}$).
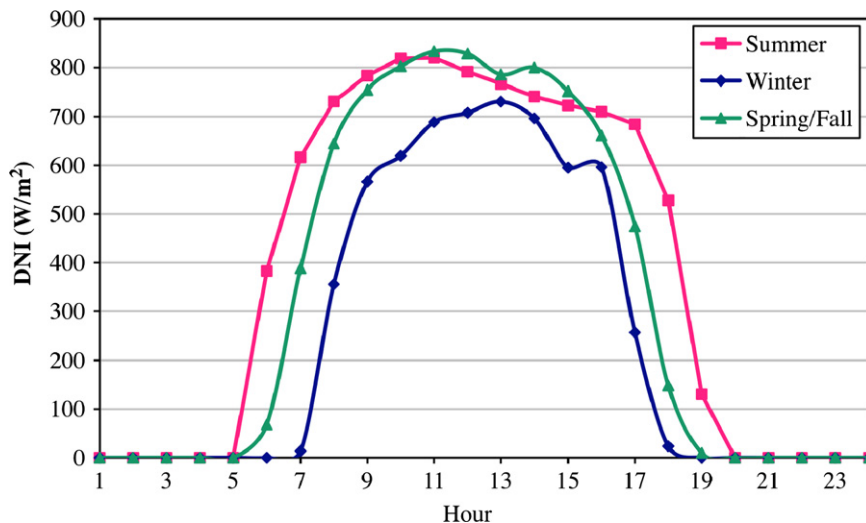

Fig. 1. Daggett Barstow (lat (N) 34.87, long (W) 116.78) hourly mean DNI for CSP operational days by season, 2005.

Table 2
Example calculation of key solar geometry parameters by season for Daggett Barstow.

Average by seasons	Summer	Winter	Spring/fall
$Hour_{noon}$ (hour)	9.6	6.6	7.4
$Hour_{daylight}$ (hour)	14.0	10.6	12.3
$DailyIrradiance$ (kWh/m^2/day)	9.2	5.9	8.0
$MinIrradiance$ (kW/m^2)	0.3	0.3	0.3
$MaxIrradiance$ (kW/m^2)	0.8	0.7	0.8
$Hour_{CSP}$ (hour)	12.3	8.8	10.5
$lowDNIDays$	2	21	15

Table 2 provides an example calculation of key solar geometry parameters by season for Daggett Barstow. We have implicitly assumed that the variance in solar radiation over time can be adequately described by the combination of seasonal irradiance curves for CSP operational days and the $lowDNIDays$ parameter. We do not consider shorter-term variations in output, thereby implicitly assuming that these can either be absorbed as part of grid operation or offset with operation of the hybrid backup capacity of the CSP plant. Further, when backup operation is estimated we assume non-operational days with low irradiance ($lowDNIDays$) are equally distributed across the seasons (see Section 2.7). This assumption could easily be relaxed with improved data on solar irradiance (see Section 4.2).

2.6. Electricity output from the CSP solar component

Electricity output from the CSP solar component is determined not only by the irradiance level, but also by CSP market penetration. We define CSP market penetration as the ratio of total CSP output within a given region to the total output from all I&P load plants. CSP output includes output from both the solar component (denoted as $CSPOutput_{solar}$) and the backup system (denoted as $CSPOutput_{backup}$), or

$$CSPOutput = CSPOutput_{backup} + CSPOutput_{solar} \qquad (2)$$

To calculate the actual CSP solar output ($CSPOutput_{solar}$), we first determine the potential CSP solar output (denoted as $PotCSPOutput_{solar}$). Potential CSP solar output depends only on the solar resource and system efficiency, while the actual CSP solar output is also determined by system demand. Because the potential solar output can exceed the I&P load demand for certain periods, without thermal storage this excess solar output is assumed to be dumped due to the inflexibility of conventional base load generators. A similar issue with respect to the large-scale deployment of PV is discussed in detail in Denholm and Margolis (2007), who note that the ability to partially de-rate base load generation could allow a larger contribution from intermittent renewables.

Potential CSP output is the area of ABCD in Fig. 2 times the net system conversion efficiency. In order to calculate the potential CSP output for each time slice (indicated by superscript i), we calculate the average hourly CSP output (denoted as $HourlyCSPOutput_{solar}^i$) and the CSP operational time (denoted as $Hour_{CSP}^i$) for each time slice, as shown in the following equation:

$$PotCSPOuput_{solar}^i = HourlyCSPOutput_{solar}^i Hour_{CSP}^i \qquad \forall i, \qquad (3)$$

where the hourly CSP output is solar irradiance for that hour times the CSP system electric generation efficiency and i represents the time slice (Table 1). We have defined the time slices in such a way that for certain time slices CSP will not be operational for this location. These times include summer morning, winter evening, and spring and fall evening.

Table 3
CSP solar output capability and operational hours by time slice: Daggett Barstow with a solar multiple of 1.07.

Time slices	R^i (%)	$Hour_{CSP}^i$	$AveSysLoad_{CSP}^i$ (%)
Summer morning (5:00–5:30)	0	0.0	45.5
Summer daytime 1 (5:30–9:00)	93	3.2	59.2
Summer daytime 2 (9:00–14:00)	107	5.0	85.7
Summer peak (14:00–17:00)	106	3.0	96.8
Summer evening (17:00–24:00)	94	1.2	99.4
Winter morning (6:00–10:00)	78	1.9	68.8
Winter daytime (10:00–17:30)	89	6.9	63.5
Winter evening (17:30–23:00)	0	0.0	67.7
Spring/fall daytime (5:00–19:30)	100	10.5	64.3
Spring/fall evening (19:30–22:00)	0	0.0	59.4

We can define a convenient indicator of CSP solar generation capability by time slice as R^i, the ratio of average hourly CSP output for time slice i over the CSP capacity (denoted as $Capacity_{CSP}$) as shown in the following equation. $Capacity_{CSP}$ is the maximum output from the CSP generator

$$R^i = \frac{HourlyCSPOutput_{solar}^i}{Capacity_{CSP}} \qquad \forall i. \qquad (4)$$

Table 3 presents the ratio R^i and CSP operational hours for each time slice using Daggett Barstow data, together with the assumed average system load as a percentage of the maximum system load for each CSP operational time slice (denoted as $AveSysLoad_{CSP}^i$) for comparison. Although the solar output mostly overlaps with the system demand, the correlation is not perfect. The highest three R ratios occur during summer daytime 2, summer peak, and spring/fall daytime while the three highest system load periods are summer evening, summer peak, and summer daytime 2. While there is a substantial overlap between peak demand and peak CSP output, the mismatch that does exist impacts CSP costs as shown below.

As part of this calculation we determine the optimal solar multiple by minimizing the levelized cost of generation (see below). The solar multiple is the ratio of the solar energy collected at the design point to the amount of solar energy required to operate the turbine at its rated gross power (Kearney and Price, 2004). A higher solar multiple increases the plant capacity factor but also increases capital cost.

Note that the optimal solar multiple in this case is 1.07, thus the R ratio can be greater than 100% for certain time slices. The actual output cannot be greater than the rated capacity, which means the excess solar output greater than the rated capacity will be wasted if there is no thermal storage. The optimal solar multiple found here is smaller than that in some other studies (Kearney and Price, 2004; Price, 2003) due to our assumption of optimal system operation instead of a fixed seasonal CSP output profile.

To calculate actual CSP solar output, we need to consider the interaction between the CSP plant and the rest of the system. Since CSP plants in this case are defined as I&P load power plants, we determine the I&P load demand for each time slice (denoted as $EDemand_{I\&P}^i$) as the average I&P load times the number of hours in a given time slice, as described in the following:

$$EDemand_{I\&P}^i = (AveSysLoad^i - Generation_{base})Hour^i \qquad \forall i. \qquad (5)$$

Similarly, we calculate the I&P load demand for each CSP operational time slice (denoted $EDemandCSP_{I\&P}^i = EDemand_{I\&P}^i$ $(Hour_{CSP}^i/Hour^i)$), which is the demand during the fraction of each time slice that the CSP plant is operational. Because supply must always equal demand, $EDemandCSP_{I\&P}^i$ is also the maximum output that CSP can produce for each CSP operational time slice (denoted as $MaxCSPOutput^i$). Any additional output that CSP

produces will be wasted. Therefore, the actual CSP output from the solar component for each time slice can be calculated as follows. This case assumes no thermal storage, an assumption that is relaxed in the following section:

$$CSPOutput_{solar}^i = \begin{cases} PotCSPOutput_{solar}^i & \text{if } PotCSPOutput^i \leq EDemandCSP_{I\&P}^i \\ EDemandCSP_{I\&P}^i & \text{otherwise} \end{cases}$$

(6)

2.7. Electricity output from the CSP backup component

Because the net conversion efficiency of gas-to-electricity in a hybrid CSP plant is lower than the efficiency of stand-alone gas turbines due to parasitic loads such as heaters and heat transfer fluid pumps (National Renewable Energy Laboratory (NREL), 2005; Leitner and Owens, 2003), under optimal operation of the electric system, CSP backup generation would be used only after stand-alone gas turbines or other available capacity has been dispatched. Here we assume that all other I&P load capacity not otherwise meeting load demand is available for backup and will be fully dispatched before the CSP backup mode is dispatched. CSP backup generation would, therefore, likely be needed not only when the electricity output from the CSP solar component is low due to low irradiance, but electric demands remain relatively high and non-CSP capacity cannot meet demand, such as summer evenings.

Under this assumption the calculation of CSP output from the backup component is straightforward. For each time slice, we first find the corresponding I&P load, and then compare this with the aggregated output level from the CSP solar component and non-CSP plants. If there is a deficit, the CSP backup mode will be dispatched to make up the deficit. The output using CSP backup mode is therefore

$$CSPOutput_{backup}^i = \begin{cases} EDemand_{I\&P}^i - CSPOutput_{solar}^i - Capacity_{nonCSP} Hour^i, \\ \text{if } EDemand_{I\&P}^i - CSPOutput_{solar}^i - \\ Capacity_{nonCSP} Hour^i \geq 0 \\ 0 \quad \text{otherwise} \end{cases}$$

(7)

In addition, when CSP plants are not operational due to low DNI days (lower than 300 W/m^2) or high wind days (greater than 35 mph) (Kearney and Price, 2004), the CSP backup mode is needed to provide output for the CSP plant. We assume that the backup amount for each time slice is the average CSP output for that season. The total annual output from the CSP backup mode is the sum of backup output at each time slice due to solar supply deficit and the backup output due to low DNI days.

High wind days are relatively rare in most locations so we ignore this effect and only consider low DNI effects. For example, for a windy site with an average wind speed of 7.75 m/s at a height of 50 meters (wind resource class 5), wind speeds greater than 15.65 m/s (35 mph) would occur only 4% of the time assuming a Rayleigh distribution for wind speed. The occurrence of high wind would likely be lower than this at ground level. For many land locations the occurrence of high wind days would be even less than this value since land wind speeds tend to peak at night when the CSP solar field is not active.

3. CSP cost and performance

3.1. CSP as I&P plants without thermal storage

The central determinant of CSP technology deployment in the long-term will be electric generation cost. We consider here the levelized energy cost (LEC) of CSP generation without

Table 4
Baseline assumptions for calculating CSP LEC (in 2004 $).

Variables	Value
Capital cost per unit of installed capacity assuming 1.07 solar multiple (c) ($/kW)	2801
Fixed O&M cost (OM_{fixed}) ($/kW-year)	47.87
Variable O&M cost ($OM_{variable}$) ($/mWh)	2.72
Price of fossil fuel natural gas ($Price_{gas}$) ($/MMBtu) (HHV)	4.65
Gas-to-electricity conversion efficiency ($Efficiency_{gas-electricity}$)	0.32
Lifetime of the plant (n)	30
Capital charge rate (CCR) (%)	9.38

consideration of environmental externalities or subsidies. LEC is an appropriate general comparison metric with respect to other generators within the same market segment (e.g. intermediate-peak or base load), because hybrid CSP plants provide firm electric power as do conventional fossil plants. The cost of fuel to supply auxiliary power is included in our definition of LEC. The effect of tax and other financial incentive policies can be considered by choosing an appropriate discount rate (Zhang and Smith, 2008).

The cost for CSP generation varies as a function of market penetration. To calculate CSP LEC we calculate backup fuel use and total CSP output at each CSP market penetration level and then use the following formula (EEL, 1999) to calculate CSP LEC. The baseline economic assumptions used are shown in Table 4 and are taken from Kearney and Price (2004) and National Renewable Energy Laboratory (NREL) (2005). The LEC is

$$LEC = \frac{CCR I + OM + F}{CSPOutput}$$

(8)

where CCR is the capital charge rate; I is the capital cost; OM is the annual operation and maintenance costs, which can be calculated as $OM = OM_{fixed} Capactiy_{CSP} + OM_{variable} CSPOutput$; and F is the annual expenses for fuel, which can be calculated as $F = Price_{gas} (CSPOutput_{backup}/Efficiency_{gas-electricity})$, where $Price_{gas}$ is the price of fossil fuel natural gas. The fixed charge rate chosen for the calculations in this section are equivalent to a simple real interest rate of 8.6% with a capital lifetime of 30 years, a value similar to that used in other studies of renewable energy.

Fig. 3 shows how CSP LEC changes with CSP market penetration for our example location in Barstow. In addition to the baseline scenario, scenarios with 80% of baseline capital cost and 50% of baseline capital cost are presented. Assuming idealized system dispatch, costs are constant at low penetration levels. This implies that substantial CSP capacity could be constructed before significant cost increases due to intermittency are encountered. Note that, while a fixed natural gas price is used in this illustrative calculation, the cost of auxiliary fuel can be endogenously calculated if this representation is embedded in a dynamic model as demonstrated below.

As CSP generators supply a larger portion of I&P power demand CSP LEC increases due to two factors: increased wasted solar output and the costs of purchasing natural gas to fuel increased backup operation as shown in Fig. 4. The addition of thermal storage to this system would mitigate this loss of output and also allow a reduction in operation of the backup system. This will potentially decrease CSP LEC, depending on the cost of the thermal storage system. The following two cases will examine CSP applications with thermal storage.

3.2. CSP as I&P plants with thermal storage

The addition of thermal storage provides a buffer to smooth variable solar output to better match the I&P load curve. While thermal storage systems are not in operational use, such systems
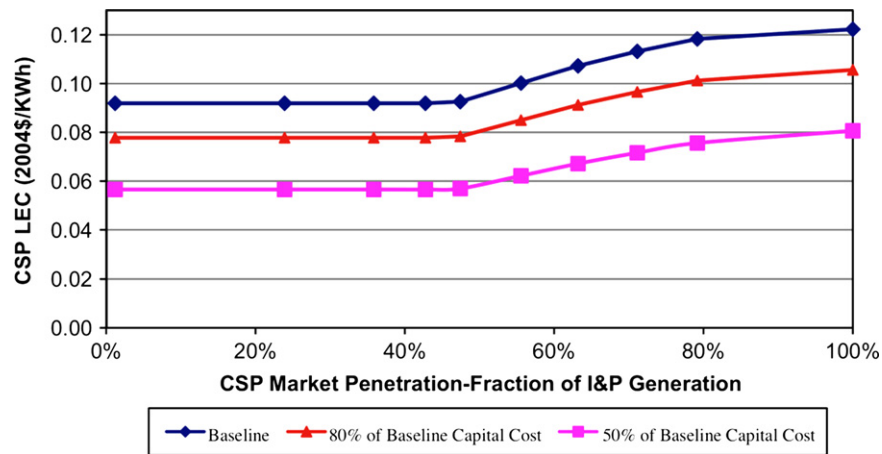
Fig. 3. CSP LEC as a function of CSP market penetration—CSP as I&P load power plants without thermal storage.
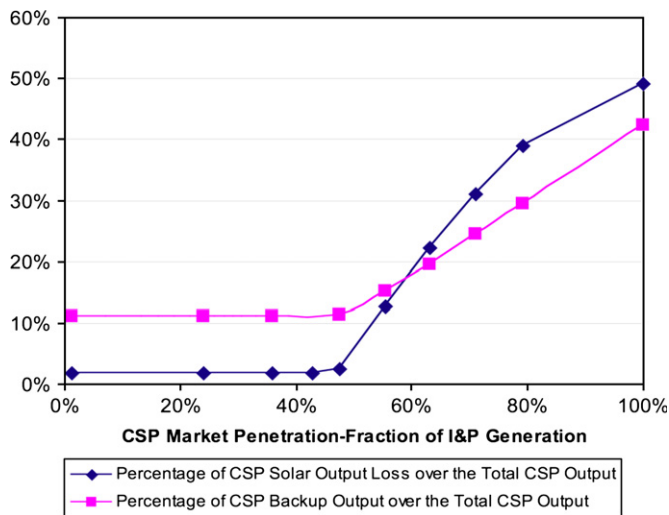

Fig. 4. Percentage of CSP output loss over the total CSP output and fraction of plant electricity produced by the backup system vs. CSP market penetration.

Fig. 5. CSP LEC as a function of CSP market penetration—CSP as I&P load power plants with thermal storage (corresponding optimal solar multiple is in Table 5).

Table 5
Optimal solar multiple by thermal storage hour.

Hours of storage	0	1	2	3	4	5	6
Solar multiple	1.07	1.15	1.15	1.25	1.35	1.55	1.65

are being developed and could be commercially viable in the future. In terms of methodology, the key addition to the calculations presented above is that for each time slice, thermal storage can potentially be used to store the solar output that: exceeds generation capacity due to an oversized solar field, exceeds the I&P demand at a specific time, or is below CSP operational requirements (irradiance level lower than 300 W/m^2). Stored solar output then can be used at any later time slice when irradiance is not available or low, particularly in evenings. We assume the order of dispatched capacity is: CSP solar output directly from solar field, heat energy drawn from thermal storage, other I&P capacity, and output from the CSP backup component. We further assume that any leftover thermal energy in storage at the end of the day will be wasted. While there may be circumstances where some energy that remained stored could be used the following day (if the storage technology used allowed this), this assumption has little impact on the results since wasted thermal energy is small for systems with thermal storage.

For thermal storage costs we assume a fixed cost of $140/kW and a variable cost of $23/kW-hour storage, derived from National Renewable Energy Laboratory (NREL) (2005). In addition, we assume that fixed O&M costs increase to $58/kW-year (National Renewable Energy Laboratory (NREL), 2005) for units with thermal storage. We denominate the amount of thermal storage
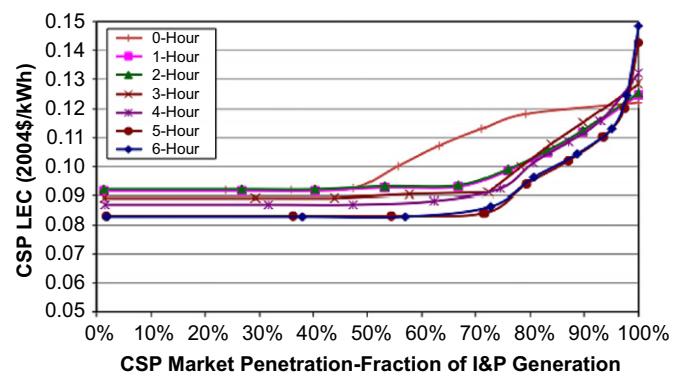
added to the plant as the number of hours of power generation at rated (turbine) capacity that can be driven by the storage system. Fig. 5 shows the results of CSP LEC as a function of CSP market penetration by the number of hours of thermal storage. The corresponding optimal solar multiple is presented in Table 5. The shape of CSP LEC versus CSP market penetration is primarily driven by increased proportions of wasted solar output, as illustrated in Fig. 6. The share of backup operation is relatively stable in this case due to availability of stored solar output. At penetration levels above 70–80%, depending on the amount of storage, costs begin to increase as some solar output is wasted in seasons where total CSP capacity exceeds I&P demand.

From Fig. 5, we can see that thermal storage extends the market penetration threshold where CSP LEC starts to increase. This is perhaps the largest benefit from the addition of thermal storage systems. The addition of thermal storage also allows CSP plants to operate into the evening without using backup fuel. The value of this capability will depend on the relative cost of thermal storage and natural gas (or biomass) fuel at any given location. In
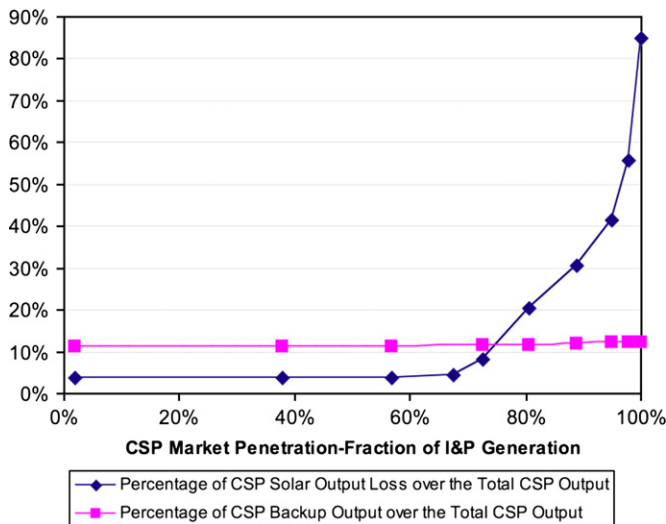
Fig. 6. Percentage of CSP output loss over the total CSP output and fraction of plant electricity produced by the backup system vs. CSP market penetration—CSP as I&P load power plants with 6-hour thermal storage.

addition, thermal storage can reduce CSP LEC (Fig. 5), because the addition of thermal storage acts to leverage fixed costs (e.g. generator and turbine) by increasing the solar multiple. However, these benefits saturate at about five hours of storage.

3.3. CSP as base load plants with thermal storage

In this section, we examine the case where CSP plants operate as base load generators. We assume that the CSP output in winter is maintained year-round as base load generation. Since DNI is higher and daylight hours are longer in summer and spring/fall than in winter, CSP generates additional I&P electricity in these seasons in addition to base load electricity. Therefore, CSP plants in this case receive revenues from serving both base and I&P loads.

In terms of methodology, the key feature of this case is that in winter, the daily solar output is smoothed through thermal storage to provide steady base load electricity, while in summer and spring/fall, in addition to providing base load electricity, the extra energy supplied by the additional solar irradiance available in these seasons can be used to meet some of the I&P load demand. Due to the relatively small share of CSP I&P load supplied from these plants, no solar output will be wasted due to exceeding I&P load demand and the CSP gas-hybrid backup generation is only needed during low DNI days. Thus, the impact of CSP market penetration on LEC is negligible for a CSP system operating as a base load plant.

Because base load CSP plants sell electricity to both I&P and base load markets, instead of an LEC we calculate and equivalent quantity: the breakeven base load electricity price at which capital an operating costs of the CSP plant are met. We assume the ratio of I&P to base load electric prices is 2, based on CA wholesale market data from Energy Information Administration (Energy Information Administration (EIA), 2008). Using this assumption, the breakeven base load electricity price for CSP is around $0.065/kWh, which is not competitive with current prices. If we assume capital costs can be reduced to 50% of the baseline values (Table 4), the breakeven base load electricity price is in about $0.04/kWh, which is competitive. Fig. 7 presents the breakeven base load price for CSP as a function of thermal storage hour. The sensitivity to the ratio of I&P load over base load price is also shown. The lowest CSP cost occurs at 10–11 hours of thermal storage, although CSP LEC is not very sensitive to either the
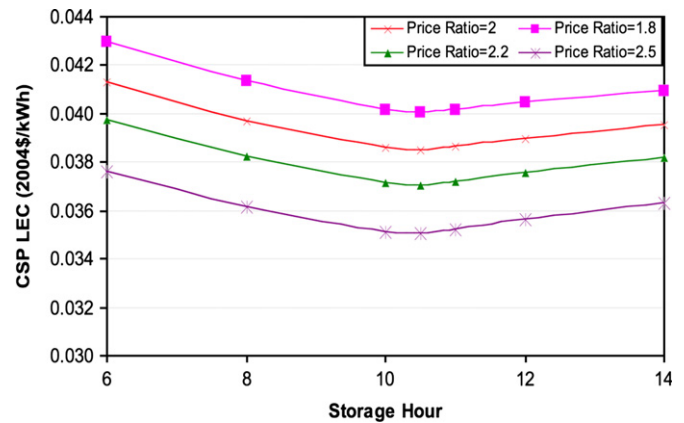

Fig. 7. CSP LEC by thermal storage hour with optimal solar multiple and 50% of baseline capital cost—CSP as base load power plants with thermal storage.

number of storage hours or the price ratio. We, therefore, find that for base load CSP operation the primary factor controlling competitiveness is CSP capital cost. The number of low DNI days is also a factor, particularly if natural gas (or biomass) prices increase in the future.

4. THE potential global role of CSP

4.1. Long-term modeling

The potential contribution of CSP electric generation technologies will depend first on the cost of CSP electric generation, which has a strong dependence on the quality of the solar resource. The role of CSP will also depend on electricity demand, the cost of other electric generation technologies, and environmental incentives such as a price on carbon. In order to examine these questions, the representation of CSP technologies described above was implemented within the GCAM (formerly MiniCAM) integrated assessment model.

While the results above were derived for one specific location, we can generalize these findings by noting that the cost and performance of CSP technologies depends largely on just two location-specific parameters, the number of low DNI days and the average irradiance on operational days. The inflection points for CSP I&P technologies where increased costs are incurred (Figs. 3 and 5) do depend on the detailed load and irradiance curves. This has little impact on our simulation results, however. The final step before we can implement a global analysis, therefore, is to estimate global solar resource parameters as described in the next section.

4.2. Global solar resource estimate

Operational day DNI and the average annual number of low DNI days were estimated using data at a one-degree spatial resolution from the National Aeronautics and Space Administration (NASA) Surface meteorology and Solar Energy dataset release 6.0[2] (e.g. Chandler et al., 2004). Neither of these quantities are available directly from this dataset, so an estimation procedure was used whereby solar properties on non-operational days were estimated using correlations between the ratio of clear-sky to total ground radiation and the necessary parameter in the US National Solar Radiation Database (NSRDB). The methodology used for this calculation is given in Appendix A.

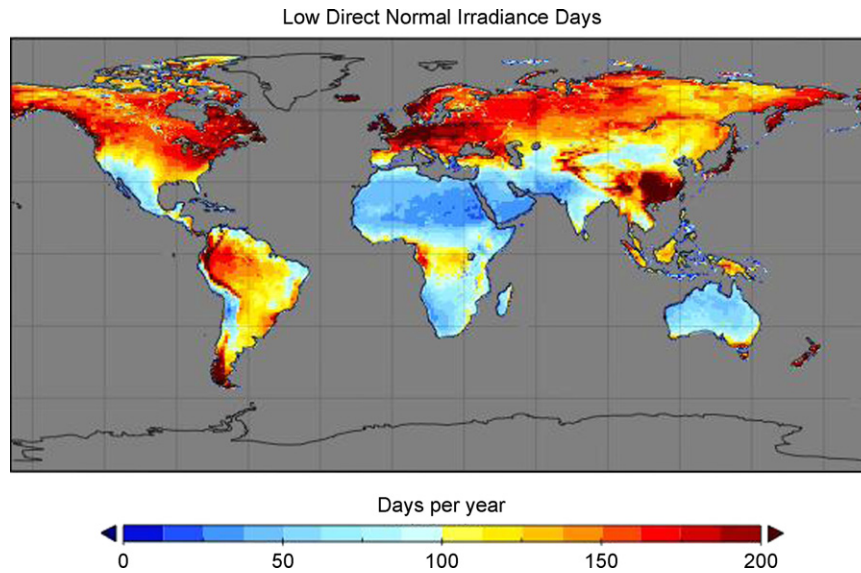[2] See http://eosweb.larc.nasa.gov/sse/.

Fig. 8. Estimate of the number of days where DNI falls below 3000 W/m^2.

Table 6
Number of days with DNI < 3000 W/m^2 for each solar class by region.

Region	Number of low DNI days					
	Class 1 (< 4.5 kWh/m^2/day)	Class 2 (4.5–5 kWh/m^2/day)	Class 3 (5–6 kWh/m^2/day)	Class 4 (6–7 kWh/m^2/day)	Class 5 (7–7.5 kWh/m^2/day)	Class 6 (> 7.5 kWh/m^2/day)
USA	–	187	126	101	71	58
Canada	–	–	181	–	–	–
Western Europe	–	–	117	103	68	61
Japan	–	190	171	124	58	–
Australia and NZ	188	181	124	54	40	34
Former Soviet Union	–	186	98	75	151	128
China	174	156	162	89	85	82
Middle East	–	186	43	31	22	13
Africa	175	107	62	30	18	14
Latin America	154	136	88	45	46	43
Southeast Asia	166	132	98	48	22	60
Eastern Europe	–	173	155	107	78	–
Korea	–	–	138	–	–	–
India	–	–	16	53	153	111

The estimated number of low DNI days for the globe is shown in Fig. 8. The light shaded regions in the figure indicate areas where the number of low DNI days is less than 100 days per year, which is a rough indicator of areas well suited for CSP technology. The number of low DNI days is an important indicator of the quality of the direct solar resource. The Middle East and North Africa have the highest quality resource, where we estimate that there are very few days where a CSP plant cannot operate. Note that these estimates are averages over relatively large regions. Specific locations in these areas can have properties that differ from large-area averages due to local meteorological effects that impact cloud cover. For use in the model calculation we aggregated the resource estimates into six categories based on the average DNI level (Table 6). Only areas with low DNI days < 200 were included, since areas where the majority of days are cloudy would not be suitable for CSP technology deployment. Forested and cropland areas are excluded.

Each of the 14 GCAM regions is divided to six geographic sub-regions, with the resource classifications and the area of land in each resource class shown in Table 7. The current SSE uses different irradiance to DNI parameterizations poleward of 45° than between 45°N and 45°S which produces a discontinuity on the global map. Since regions poleward of 45° are generally not well suited for CSP power, these areas are excluded from this study and have little impact on the results.

A key feature of the solar resource in many world regions is its geographic concentration. In the United States, for example, the highest quality solar resource is found in the southwestern portion of the country (e.g. Blair et al., 2006). For the calculations presented here, we make a conservative assumption where we treat each solar resource class as a separate sub-region for purposes of estimating CSP technology characteristics and parameters such as the fraction of system load supplied by CSP. We make the assumption that each solar resource class is spatially continuous enough that we can treat all loads within that region together. This is generally true for the higher quality solar resources where CSP has the most potential.

4.3. The potential role of CSP

We now combine the representation of CSP technologies developed in the first portion of this paper with the solar resource

Table 7
Area for each solar class by region.

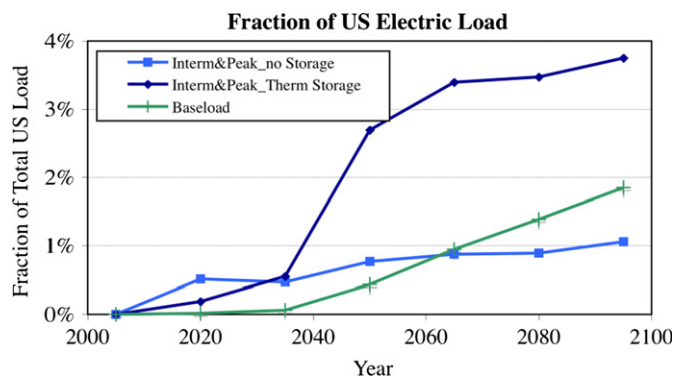| Region	Area (km²)					
	Class 1 (< 4.5 kWh/m²/day)	Class 2 (4.5–5 kWh/m²/day)	Class 3 (5–6 kWh/m²/day)	Class 4 (6–7 kWh/m²/day)	Class 5 (7–7.5 kWh/m²/day)	Class 6 (> 7.5 kWh/m²/day)
USA	–	264	2773	113,541	227,257	168,091
Canada	–	–	380	–	–	–
Western Europe	–	–	8569	12,655	12,207	10,648
Japan	–	1824	850	145	0	–
Australia and NZ	369	14	6608	289,338	850,751	3,843,693
Former Soviet Union	–	115	197,911	267,215	17,612	9805
China	943	1014	11,829	726,966	479,398	439,120
Middle East	–	277	5212	304,777	970,911	1,498,909
Africa	49	8121	362,691	1,455,713	2,080,459	5,225,091
Latin America	956	3431	39,001	77,048	134,637	83,467
Southeast Asia	15,459	36,239	65,507	160,462	162,515	11,717
Eastern Europe	–	156	450	93	56	–
Korea	–	–	1339	–	–	–
India	–	–	35,142	51,337	20,002	18,071

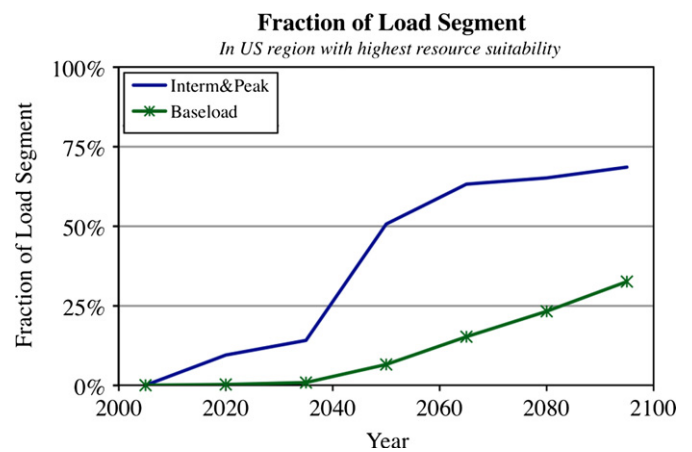**Fig. 9.** Fraction of US electric load supplied by CSP technologies.

Fig. 10. Fraction of load segment served in the US region with high resource suitability (most of inland California, Nevada, Arizona, New Mexico, and southwest Utah).

estimates developed above in order to evaluate the potential role of CSP technologies in the US and global energy system. The CSP representation above was implemented in the GCAM integrated assessment model. A brief description of the GCAM model and a description of the implementation of CSP technologies in the model are provided in Appendix A.

Fig. 9 shows GCAM model results for CSP market penetration in the US under a reference case scenario derived from Clarke et al. (2007). CSP plant capital costs were assumed to decrease at a rate of roughly 0.6% per year. This represents a reference technology case with continued incremental reductions, but without the type of focused research effort that would result in more rapid cost decreases, for example as assumed in one recent analysis (NREL, 2007a).

The largest role for CSP for the first half of the century is to supply intermediate and peak loads. In the near-term, CSP plants without thermal storage are competitive as their penetration is not sufficient to suffer penalties due to lost solar output or increased backup mode operation. As penetration increases and I&P plants with thermal storage are fully developed, these become the preferred option as thermal storage allows these plants to serve a higher fraction of I&P load without increased operation of the backup mode.

As CSP technology costs fall, CSP becomes more competitive for base load generation as well. The potential for CSP base load is ultimately larger due to a larger market segment and the absence of significant penalties at higher penetration levels.

Fig. 10 shows the dynamics of CSP in this model for those US regions with the highest resource suitability (our classes 5 and 6, which are in the west and southwest of the US). Note that these results must be interpreted with some caution since neither electricity supply and demand within each sub-region nor separate peak, intermediate, and base load markets were explicitly modeled, although some of these simplifying assumptions will be addressed in future work. However, the impacts of increasing CSP penetration do reflect the dynamics derived earlier in this paper. By mid-century CSP is providing the majority of intermediate and peak demand in these regions. The CSP contribution peaks at about 70% due to the cost of operating hybrid mode and lost output that would be incurred beyond this point. The fraction of base load demand supplied by CSP steadily increases over time as costs fall. After 2050 most of the growth in CSP output is due to additional base load generation.

Fig. 11 shows CSP generation by world region while Fig. 12 shows CSP generation as a fraction of total electric generation. All regions show some level of CSP generation. At very low penetration levels this is a result of the logit sharing algorithm used in this model (Clarke and Edmonds, 1993), where even high cost options have some market share. The Middle East, India, and Africa have the highest penetration rates, with the higher penetration in India is due to somewhat higher electricity prices
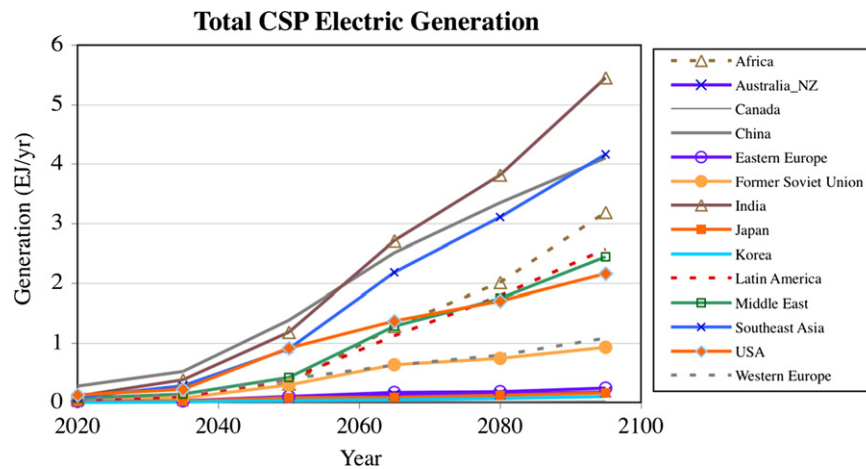
Total CSP Electric Generation

Fig. 11. Total CSP generation by region.

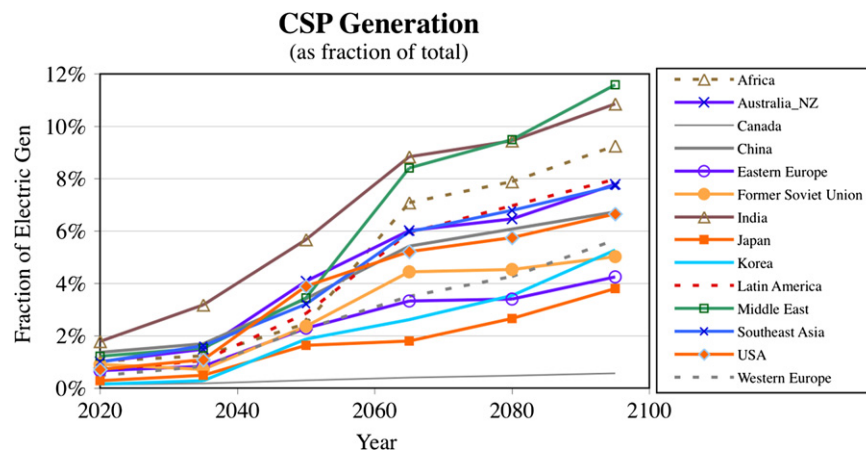## CSP Generation
(as fraction of total)

Fig. 12. Fraction of regional electric load served by CSP.

in this region making CSP competitive even though low DNI days are relatively large (Fig. 8). A second group of regions with moderately large fractions of CSP include Latin America, Australia and New Zealand, South and East Asia and the United States. All of these regions have areas that contain good solar resources. In all the above cases, an additional assumption of enhanced transmission infrastructure (not assumed here) would allow a larger expansion of CSP technologies. The remaining regions (Former Soviet Union, Europe, Canada, Japan, and Korea) have relatively poor resources for CSP, although as indicated in these results there are some locations where CSP generation may be competitive.

CSP supplies 4% of US electric generation in 2050 in this scenario. For the only comparable published study on this time scale, the central case of Blair et al. (2006) results in a CSP capacity 55 GW in 2050, or about 2.75% of total US generation capacity. On an aggregate level, the representation developed here produces results broadly comparable to the more spatially and temporally detailed representation in Blair et al. (2006). The contribution of CSP technologies is much larger here than the aggregate solar technology included in a previous version of the same model (Clarke et al., 2007), where only 1% of US electric demand was supplied by solar in 2050.

Fuel costs for hybrid backup operation on low DNI days can be a significant portion of total generation costs, particularly later in the century. In early time periods, backup costs are very low, 2–4%

of total cost, in regions with exceptionally good resources such as the Middle East, and 7–8% in the US Southwest. Later in the century backup costs can increase significantly, often reaching 20% of total costs in the US Southwest. This increase is due to two factors. First, CSP capital costs are assumed to fall over time while the need for backup operation does not decrease. Second, backup in these scenarios was assumed to be supplied by either natural gas or biomass and the costs of both of these fuels increase over the century in our reference case. If a more aggressive decrease in CSP capital costs over time were assumed, the fuel costs for hybrid backup operation would be an even larger fraction of the total generation cost for CSP technologies.

The CSP technology assumptions used here implicitly assume significant water use for the steam turbines, largely for cooling (Sargent and Lundy, 2003; Department of Energy, 2008). Restrictions on water use in the arid regions that often have the most appropriate solar resources for CSP would change the net plant efficiency and costs assumed here if dry-cooling technologies were implemented. Power-tower CSP plants, which have a lower efficiency penalty for dry cooling due to their higher operating temperature, could become the preferred option in these situations (Department of Energy, 2008). Hybrid cooling systems would allow even parabolic trough plants to operate with only a few percent loss in overall output, albeit with a modest increase in cost (Department of Energy, 2008). Power tower plants with much higher operating temperatures might some day allow the

use of gas turbines, perhaps eliminating the need for cooling entirely (Heller et al., 2006; Angelino and Invernizzi, 2008).

5. Discussion

Analysis results that provide insights into the potential role of new technologies are a key aid for policy formation. In this paper we have developed a methodology that enables CSP technologies to be incorporated into energy-economic analysis. We find that, assuming modest improvements in capital costs, CSP technologies have the potential to supply a significant portion of electric demands in favorable regions.

We examined three potential applications of CSP electric generation technologies: (1) CSP as intermediate and peak (I&P) load power plants without thermal storage, (2) CSP as I&P load power plants with thermal storage, and (3) CSP as base load power plants with thermal storage. We find that, for the capital cost assumptions used here, CSP plants without thermal storage can be competitive as I&P load plants in prime locations. Either policy incentives, lower capital costs or high natural gas prices could result in electricity generation that is competitive with natural gas turbines. For our example location, CSP plants can serve around 40% of the I&P load without suffering a penalty due to mismatch between generation and demand under an assumption of optimal system operation. Significant expansion of current CSP technology in areas with applicable resources is, therefore, potentially feasible.

The increase in generation cost after a certain threshold is partly due to the increasing need for operation of the auxiliary backup system and partly due to the loss of CSP output from the solar component when there is excess supply. Because of this increased use of natural-gas backup, the usefulness of CSP plants to reduce carbon emissions from I&P generation decreases at high penetration levels. Operation in backup mode, however, increases revenues and would allow capacity payments to the CSP plant operator.

The development and successful deployment of reliable, cost-effective thermal storage technology enhances the performance of CSP plants operated to serve I&P load by extending the amount of I&P load that can be cost-effectively served without penalty due to solar intermittency. Even a few hours of thermal storage are sufficient to allow CSP plants to serve up to around 70% of the I&P load without penalty. Otherwise wasted solar output can now be stored, which can then be used in early evening when electric demand is still high, which also reduces, but does not eliminate, the need for gas-fired hybrid backup operation. Increasing storage capacity up to 5 hours also results in a modest reduction of the total levelized cost.

If sufficient cost reductions can be gained through the development and deployment of CSP technologies as I&P plants then CSP plants could then competitively supply base load electricity. While the deployment of CSP plants to supply base load power could result in a much larger application of CSP technology, this also requires not only the deployment of long-lasting thermal storage but, in order to produce electricity at a competitive price, this also will require significant reductions in capital costs.

Current modeling studies often include CSP technologies with thermal storage supplying I&P loads by making an assumption of firm power generation (Blair et al., 2006; Lew et al., 2009). Our results support this general approach, at least for sunny days and penetration levels less than about 70% (Fig. 6). It appears, however, that backup operation on cloudy days when the CSP system cannot operate is not explicitly considered in previous studies. We find that costs for hybrid backup operation in the US Southwest increase from 7% to 8% of total system costs currently up to 20% of total system costs by the end of the century. By mid-century these costs are largely due to operation on low DNI days when the CSP solar field is not operating, if we assume the cost-effective deployment of thermal storage. Furthermore, we also find substantial CSP penetration in some regions, such as India (Figs. 11 and 12), that have a relatively large number of low DNI days. In these regions CSP is operating as a fuel extending technology, and an even larger fraction of the total cost is due to backup operation. Even so, we find that CSP technology becomes competitive in these regions as fuel prices increase.

Given that CSP technology is most viable in areas with a large number of clear days, accurate information on solar resources is necessary to evaluate the potential for this technology. We found that current data products were not fully adequate for assessing CSP viability. New data sets estimating the number of low DNI days where the CSP solar field would not be operational, and the average irradiance for days in operation were developed (these data sets are available from the authors). Instead of persistence, which is currently reported in the NSRDB, we find that CSP operation costs are better parameterized by the total number of days with low direct normal irradiance, which is the primary determinant of the need for backup mode operation. Further, the relevant parameter for CSP operation is not average direct irradiance but direct irradiance on operational days where total irradiance is above a threshold value. We recommend that estimates of these quantities be improved and made available for analytic studies.

Thermal storage systems can only supply firm power for specified periods, which might include evening hours, short cloudy periods during a day, or overnight in the case of base load systems. Thermal storage cannot fulfill the role of supplying backup power for days in which direct irradiance is not sufficient to operate the CSP solar field. We find, however, that costs for operation of CSP backup mode become an increasing component of total system costs in the future. It is important, therefore, that more analysis of the role of hybrid backup operation in CSP plants within an integrated systems context is conducted, particularly at higher penetration levels. Detailed system simulations using measured or simulated data for irradiance and other relevant parameters such as those of Lew et al. (2009) could be very helpful in this respect if extended to include higher penetration levels for CSP plants.

Acknowledgments

Appendix A

A.1. Global solar resource methodology

The number of low DNI days is not available from the NASA data, so this quantity was estimated by developing a correlation

between the NASA data and the number of low DNI days for 16 continental stations reported in the US National Solar Radiation Database (NSRDB). We determined that the most appropriate quantity in the NASA data was the ratio of clear-sky to total ground radiation, which is a measure of the effect of clouds. The number of low DNI days for these 16 sites on a monthly basis in the continental US was estimated from the NSRDB data from 1991 to 2005 using a threshold for direct normal radiation of 3000 Wh/m^2. The total number of low DNI days for these sites was estimated from the NSRDB persistence report, assuming that persistence runs greater than 15 consecutive days were equal to 15 (unless all days in the month were cloudy). The sites were selected to be sufficiently separated such that they were judged to be independent estimates. The SSE clear-sky/ground radiation ratio correlates reasonably well with the number of low DNI days as estimated from the NSRDB persistence files, with a correlation coefficient $r^2 = 0.72$.

Adding data from several island stations (Hawaii, Puerto Rico, and Guam) noticeably degraded the correlation so data from these stations were not used. This may be due to the fact that the station data are point estimates that may be strongly influenced by local coastal effects at these island stations while the NASA data represent regional averages over a relatively large grid cell. Another possibility is that the correlation coefficients may be different for tropical regions. Further work is needed to more directly estimate the number of low DNI days from measurement and assimilation data, but this is beyond the scope of this project.

An estimate of the irradiance level during CSP operational days when solar irradiance is above 3000 Wh/m^2 is also needed. Only monthly total direct irradiance is available from the NASA dataset. This means that an approximation procedure is also needed to estimate operational day irradiance. It is expected that improved procedures now being implemented in the NASA SSE dataset should allow a direct calculation in the future. The irradiance during operational days is estimated by subtracting total irradiance during low DNI days from total irradiance for each month. The annual average DNI value during operational days used here is the average of the 12 monthly values. Irradiance during low DNI days was estimated using a correlation developed using the NSRDB database using a similar procedure as used to estimate the number of lowDNIDays. We find that the average irradiance during low DNI days is inversely correlated with cloudiness (the ratio of clear-sky to total ground radiation), although the correlation has significant scatter with a correlation coefficient $r^2 = 0.51$. For a few locations the maximum irradiance during operational days was unrealistically high for some months. The maximum monthly operational day DNI in such instances was set to 10 kWh/m^2/day. In a few sub-regions (China classes 3–6, FSU and SE Asia classes 5–6, and USA class 2) the resulting annual average was anomalously large in comparison with other regions and an average value for that solar class was used instead.

A.2. GCAM model description

The GCAM is implemented within the Object-oriented Energy, Climate, and Technology Systems (ObjECTS) framework which is a flexible, object-oriented modeling structure (Kim et al., 2006). The GCAM is a partial-equilibrium, integrated model of the economy, energy supply and demand technologies, agriculture, land-use, carbon-cycle, and climate. This framework is intended to bridge the gap between "bottom-up" technology models and "top-down" macro-economic models. By allowing a greater level of detail where needed, while still allowing interaction between all model components, the ObjECTS framework allows a high degree

of technological detail while retaining system-level feedbacks and interactions. By using object-oriented programming techniques (Kim et al., 2006), the model is structured to be data-driven, which means that new model configurations can be created by changing only input data, without changing the underlying model code.

The GCAM is a partial-equilibrium model structure that is designed to examine long-term, large-scale changes in global and regional energy systems. The model has a strong focus on energy supply technologies and has been recently expanded to include a suite of end-use technologies. The GCAM was one of the models used to generate the Intergovernmental Panel on Climate Change (IPCC) SRES scenarios (Nakicenovic and Swart, 2000). This model has been used in a number of national and international assessment and modeling activities such as the Energy Modeling Forum (EMF) (Edmonds et al., 2004; Smith and Wigley, 2006), the US Climate Change Technology Program (CCTP; Clarke et al., 2006), and the US Climate Change Science Program (CCSP; Clarke et al., 2007) and IPCC assessment reports.

The GCAM is calibrated to 1990 and 2005 and operates in 15-year time steps to the year 2095. It takes inputs such as labor productivity growth, population, fossil and non-fossil fuel resources, energy technology characteristics, and productivity growth rates and generates outputs of energy supplies and demands by fuel (such as oil and gas) and energy carriers (such as electricity), agricultural supplies and demands, emissions of greenhouse gases (carbon dioxide, CO_2; methane, CH_4; nitrous oxide, N_2O), and emissions of other radiatively important compounds (sulfur dioxide, SO_2; nitrogen oxides, NO_X; carbon monoxide, CO; volatile organic compounds, VOC; organic carbon aerosols, OC; black carbon aerosols, BC; see Smith and Wigley, 2006). The model has its roots in Edmonds and Reilly (1985), and has been continuously updated (Edmonds et al., 1996; Kim et al., 2006). GCAM also incorporates MAGICC, a model of the carbon cycle, atmospheric processes, and global climate change (Raper et al., 1996; Wigley and Raper, 1992).

A.3. The implementation of CSP in the GCAM

The analysis of CSP resources presented in the first section of this paper relies on estimates of daily and seasonal direct solar irradiance and seasonal electric load curves. A parameterized version of the above analysis results have been implemented within a research version of the GCAM as outlined in Fig. A1 below. The implementation includes three major parts: (1) a number of solar resource classes as described in Section 4, (2) CSP technology classes that use the solar resource to supply electricity, and (3) backup mode operation of the CSP technologies using natural gas or biomass.

For each solar resource category, there are three applications of CSP technologies: CSP as I&P load power plants without thermal storage, CSP as I&P load power plants with thermal storage, and CSP as base load plants with thermal storage. Each CSP technology has three cost components: generation cost, backup cost, and grid connection cost. Backup costs consist of market prices for fuel consumption and the marginal costs of specific backup technologies. Natural gas and solid biomass fuels are implemented as separate backup technologies, with endogenous choice between backup fuel depending on cost.

We assume that approximately 15% of the total electric load is intermediate and peak load, a figure derived from a composite United States load curve, taking intermediate and peak load to occur largely during daytime and summer evenings. The performance of CSP technologies in terms of solar energy dumped and backup fuel consumed (Figs. 4 and 5) are parameterized as a
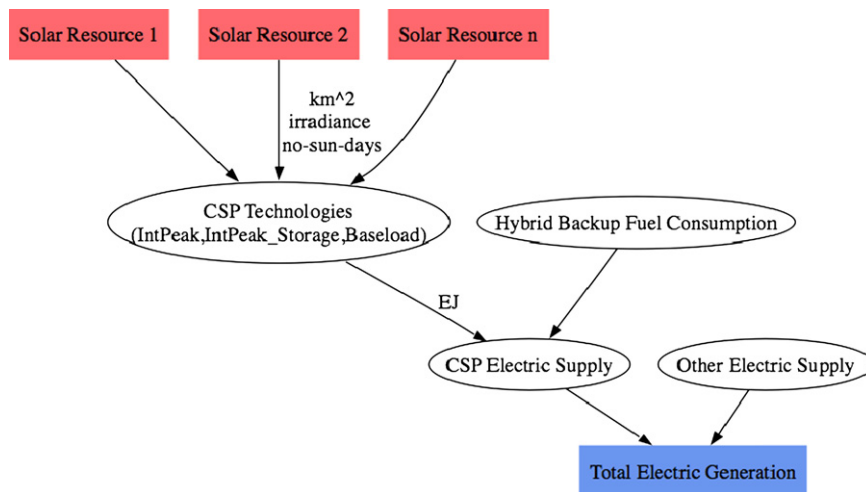
Fig. A1. Implementation of CSP in the GCAM.

function of penetration level as

$$Backup\_Fuel\_Consumption = Low\_DNI\_Day\_Consumption + \alpha \, penetration^g,$$

$$Solar\_Energy\_Dumped = \beta \, penetration^h. \tag{9}$$

The parameters α and β are set equal to the values for 100% penetration as determined by the previous analysis (Figs. 4 and 6), and the exponents η and γ are determined through least-squares curve fitting. As discussed previously, backup model fuel consumption consists of two portions: a portion due to the occurrence of low DNI days, which is assumed to be independent of penetration, and a portion that increases with increasing penetration. For operation as base load plants with thermal storage only the low DNI day component is applicable.

Since CSP technologies are not in widespread use today we must choose when this technology is mature and allowed to compete on a level basis with all other electric generating technologies. A number of CSP I&P plants without thermal storage are either under construction or planned so we assume that this technology is mature by 2020. No full-scale CSP I&P plants with thermal storage are currently operating so we assume this technology is competitive by 2035 and fully mature by 2050. CSP base load plants are competitive in the 2035–2050 time frame and fully mature by 2065.

Note that, while electric transmission grids do not currently serve large portions of some developing regions, the simulations considered extend over the entire 21st century. At the points where CSP technologies become widespread in these simulations, it is reasonable to assume that electric transmission infrastructures will have been largely deployed in most of these regions.

The GCAM model does not include an explicit representation of regional electric markets at a level of detail lower than the 14 regions shown in Table 6. In order to account for the heterogeneous resource base for CSP, CSP technologies were implemented for each of the six solar classes in each model region. The GCAM model provides electric demand for the entire region, and total electricity demand within each sub-region is assumed to be proportional to population, such that the total sub-regional electricity demand is equal to the regional demand times the fraction of population within each sub-region in the year 2000. The load fraction variable needed to define CSP performance and backup requirements (Figs. 3–5) is then the amount of electricity supplied by CSP in each sub-region divided by the estimated sub-regional electricity demand. As generation of CSP in each sub-region increases, costs increase (Figs. 3 and 5) which acts to

limit CSP generation for that sub-region. For simplicity same solar multiple was used for each solar class. Capital costs, however, vary with solar class as a larger solar field is needed to provide the same thermal input to the power block as average irradiance decreases. This is not a large effect, however, as irradiance on operational (sunny) days does not vary too much between solar classes—by 20% from our class 1 to class 6. The primary difference between solar classes is the number of low DNI days.

An examination of the geographic extent of the six solar resource areas indicated that the two highest quality solar resource classes (classes 5 and 6 in Table 6) are geographically proximate so these two areas were combined for purposes of determining the maximum fraction of the regional electric load that could be served by CSP plants in these regions. Increasing this fraction would be one way of representing the potential impact of advanced electric transmission grid technologies, which would allow power transmission across a larger area within a region.

Two changes were made to the parameters used in the previous section in order to assure that CSP technology calculations in the model were performed with the same parameters used for fossil energy technologies. First, the fixed charge rate used for determining levelized cost of CSP was set to 0.125, the value used for fossil energy technologies. This is slightly higher than the value often used in renewable energy calculations. In essence, we assume that capital cost financing is provided at similar terms for all electric generation technologies. Further, similar to fossil energy technologies, we assume that 10% of the time plants are down for scheduled maintenance. We assume, however, that half of this maintenance can be conducted during low DNI days, meaning that the overall capacity factor of the CSP plant is decreased by only 5% due to scheduled maintenance. This fraction was applied equally to hybrid backup operation on low DNI days and operational days. A better estimate of maintenance requirements for CSP plants will need to be determined once a sufficient number of full-scale plants are in operation.

Our model implementation also calculates the costs of building transmission lines to connect CSP plants with the transmission grid. For the United States we calculate the distribution within each solar resource class of the distance from each grid cell to the existing transmission grid. This allows the model to estimate the cost of connecting new CSP plants to the transmission grid. In general, land with good solar resources is plentiful enough relative to the footprint of the CSP plant that this is a small portion of the total generation cost. This is in contrast to wind where access to the transmission grid cost can be a more important factor (Kyle et al., 2007). We therefore use an

approximation procedure for other world regions where we lack data on the location of the transmission grid. For regions other than the United States we used the observed statistical relationship within each solar resource class of distance to grid for the United States to approximate this relationship for solar data outside of the United States. For the US, we found that the statistical properties of distance to grid depend strongly on population density. High population density grid cells were, as expected, relatively close to the transmission grid, whereas the probability of being located at a larger distance from the grid increased as population density decreased. To approximate distance to grid in other regions we used the observed relationship in the US for other regions, scaling the overall distance to grid with the square root of the area of each region. This provides consistent estimates for all world regions. While the actual distribution of electric transmission capability may well differ from that estimated here, the impact of this assumption on the final results is small.

References

Angelino, G., Invernizzi, C., 2008. Binary conversion cycles for concentrating solar power technology. Solar Energy 82, 637–647.

Blair, N., Mehos, M., Short, W., Heimiller, D., 2006. Concentrating solar deployment system (CSDS)—a new model for estimating US concentrating solar power (CSP) market potential. In: Proceedings of the Solar 2006 Conference, 9–13 July 2006, Denver, Colorado.

California Energy Commission (CEC), 2003. CEC HELM model peak load estimates by end-use. Data obtained through Personal communication (e-mail). Data combined with JGCRI estimates of end-use by seasons.

Chandler, William S., Whitlock, C.H., Stackhouse Jr., P.W., 2004. NASA climatological data for renewable energy assessment. Journal of Solar Energy Engineering 126 (3), 945–949.

Clarke, J.F., Edmonds, J.A., 1993. Modeling energy technologies in a competitive market. Energy Economics, 123–129.

Clarke, L.E., Wise, M.A., Lurz, J.P., Placet, M., Smith, S.J., Izaurralde, R.C., Thomson, A.M., Kim, S.H., 2006. Technology and Climate Change Mitigation: A Scenario Analysis, PNNL-16078.

Clarke, L., Edmonds, J., Jacoby, J., Pitcher, H., Reilly, J., Richels, R., 2007. Scenarios of greenhouse gas emissions and atmospheric concentrations. Report by the US Climate Change Science Program and approved by the Climate Change Science Program Product Development Advisory Committee (United States Global Change Research Program, Washington, DC).

Denholm, P., Margolis, R., 2007. Evaluating the limits of solar photovoltaics (PV) in traditional electric power systems. Energy Policy 35, 2852–2861.

Department of Energy, 2008. Concentrating Solar Power Commercial Application Study: Reducing Water Consumption of Concentrating Solar Power Electricity Generation (Report to Congress).

Edmonds, J., Reilly, J., 1985. Global Energy: Assessing the Future. Oxford University Press, Oxford, United Kingdom.

Edmonds, J.A., Clarke, J.F., Dooley, J.J., Kim, S.H., Smith, S.J., 2004. Modeling greenhouse gas energy technology responses to climate change. Energy 29 (9–10), 1529–1536.

Edmonds, J.A., Wise, M., Pitcher, H., Richels, R., Wigley, T., MacCracken, C., 1996. An integrated assessment of climate change and the accelerated introduction of advanced energy technologies: an application of GCAM 1.0. Mitigation and Adaptation Strategies for Global Change 1 (4), 311–339.

Emerging Energy Research (EER), 2006. Concentrated Solar Power Heats Up. Emerging Energy Research Market Brief on Solar CSP.

Energy Efficiency and Renewable Energy (EERE), 1997. Renewable Energy Technology Characterizations. Topical Report TR-109496, Energy Efficiency and Renewable Energy (EERE), US Department of Energy ⟨http://www.nrel.gov/docs/gen/fy98/24496.pdf⟩.

Energy Information Administration (EIA), 2008. Wholesale Market Data ⟨http://www.eia.doe.gov/cneaf/electricity/wholesale/wholesale.html⟩ Date of the website access: February 22, 2008.

Enermodal Engineering Ltd. (EEL), 1999. Final report prepared for the World Bank: Cost Reduction Study for Solar Thermal Power Plants. World Bank, Washington, DC ⟨http://www.p2pays.org/ref/18/17974.pdf⟩.

Heller, P., Pfänder, M., Denk, T., Tellez, F., Valverde, A., Fernandez, J., Ring, A., 2006. Test and evaluation of a solar powered gas turbine system. Solar Energy 82 (7), 637–647.

Kearney, D., Price, H., 2004. Recent advances in parabolic trough solar power plant technology. Manuscript from the authors. An older version of the paper with the same name is available at Journal of Solar Energy Engineering, May 2002, 124(2), 109–125.

Kim, S.H., Edmonds, J.A., Lurz, J., Smith, S.J., Wise, M.A., 2006. Hybrid modeling of energy-environment policies: reconciling bottom-up and top-down. The Energy Journal.

Kyle, P., Smith, S.J., Wise, M.A., Lurz, J.P., Barrie, D., 2007. Long-Term Modeling of Wind Energy in the United States, PNNL-16316.

Leitner, A., Owens, B., 2003. Brighter than a Hundred Suns: Solar Power for the Southwest. NBEL Subcontract Report NREL/SR-550-33233.

Lew, D., Milligan, M., Jordan, G., Freeman, L., Miller, N., Clark, K., Piwko, R., 2009. How do Wind and Solar Power Affect Grid Operations: The Western Wind and Solar Integration Study (NREL/CP-550-46517).

Nakicenovic, N., Swart, R. (Eds.), 2000. Special Report on Emissions Scenarios. Cambridge University Press, Cambridge, UK.

National Renewable Energy Laboratory (NREL), 2005. Potential for Renewable Energy in the San Diego Region, Appendix E, August 2005 ⟨http://www.renewablesg.org/docs/Web/AppendixE.pdf⟩.

National Renewable Energy Laboratory (NREL), 2007a. Projected Benefits of Federal Energy Efficiency and Renewable Energy Programs: FY 2008 Budget Request, Appendix D—Solar Energy Technologies Program. Technical Report NREL/TP-640-41347. ⟨http://www1.eere.energy.gov/ba/pdfs/41347.pdf⟩.

National Renewable Energy Laboratory (NREL), 2007b. National Solar Radiation Data Base ⟨http://rredc.nrel.gov/solar/old_data/nsrdb/⟩ Date of the website access: November, 2007.

Price, H., 2003. A parabolic trough solar power plant simulation model. ISES 2003 International Solar Energy Conference Paper, NREL/CP-550-33209.

Raper, S.C.B., Wigley, T.M.L., Warrick, R.A., 1996. Global sea level rise: past and future. In: Milliman, J.D., Haq, B.U. (Eds.), Sea-Level Rise and Coastal Subsidence: Causes, Consequences and Strategies. Kluwer Academic Publishers, pp. 11–45.

Sargent & Lundy LLC Consulting Group (S&L), 2003. Assessment of Parabolic Trough and Power Tower Solar Technology Cost and Performance Forecasts, NREL/SR-550-34440.

Smith, S.J., Wigley, T.M.L., 2006. Multi-gas forcing stabilization with the GCAM. The Energy Journal Special Issue #3.

Trieb, F., Müller-Steinhagen, H., 2008. Concentrating solar power for seawater desalination in the Middle East and North Africa. Desalination 220, 165–183.

Wigley, T.M.L., Raper, S.C.B., 1992. Implications for climate and sea-level of revised IPCC emissions scenarios. Nature 357 (6376), 293–300.

Zhang, Y., Smith, S., 2008. Long-term modeling of solar energy: analysis of CSP and PV technologies. Pacific Northwest National Laboratory Report PNNL-16727.